Novel Method for Magnetic Flux Density Estimation in the Vicinity of Multi-Circuit Overhead Transmission Lines

ADNAN MUJEZINOVIC⁰, (Member, IEEE), EMIR TURAJLIC, (Member, IEEE), AJDIN ALIHODZIC⁰, (Member, IEEE), NEDIS DAUTBASIC, AND MAJA MUFTIC DEDOVIC

Faculty of Electrical Engineering, University of Sarajevo, 71000 Sarajevo, Bosnia and Herzegovina

Corresponding author: Adnan Mujezinovic (adnan.mujezinovic@etf.unsa.ba)

ABSTRACT In this paper, a novel method for the magnetic flux density estimation in the vicinity of multi-circuit overhead transmission lines is proposed. The proposed method is based on a fully connected feed-forward artificial neural network model that is trained to estimate the magnetic flux density vector components for a range of single-circuit overhead transmission lines. The proposed algorithm is able to simplify estimation process in instances when there are two or more geometrically identical circuits present in the multi-circuit overhead transmission line. In such instances, artificial neural network model is employed to estimate the magnetic flux density distribution over a considered lateral profile for only one of such circuits. The magnetic flux density estimates of the other geometrically identical circuits are derived from these results. The proposed methodology defines the resultant magnetic flux density for the multi-circuit overhead transmission line in terms of the contributions made by individual circuits. The application of the proposed magnetic flux density estimation method is demonstrated on several multi-circuit configurations of overhead transmission lines. The performance of the proposed method is compared with the Biot-Savart law based method calculation results as well as with field measurement results.

INDEX TERMS Artificial neural network (ANN), Biot-Savart (BS) law based method, current intensity, magnetic flux density, multi-circuit overhead transmission lines.

I. INTRODUCTION

The effects of low-frequency magnetic fields on the health of people that reside and/or work near overhead transmission lines have been of research interest for several decades. During this period, a number of studies were conducted with the aim of establishing how the exposures to these fields exactly affect the human body. Although these studies have shown that there is a definite association between the exposure to low-frequency magnetic fields and the development of severe human disease, some questions regarding the effects of long-term exposures to these fields on human health remain unanswered [1]–[6]. As a result of decades of research into the effects of low-frequency electric and magnetic fields on humans, the International Agency for Research on Cancer (IARC) has classified extremely low-frequency magnetic fields as possibly carcinogenic to humans [7]. The International Commission on Non-Ionizing Radiation Protection (ICNIRP) in 2010, issued guidelines for limiting electric and magnetic fields in the frequency range from 1 Hz to 100 kHz. According to these guidelines the reference levels are 1 mT for occupational exposure to 50 Hz magnetic fields and 0.2 mT for general public exposure [8]. The principal objective of these recommendations is to limit the electric currents that are induced in the human body as a result of exposure to such fields and to ensure that the induced currents do not exceed the electrical currents that are naturally generated by the human nervous system and heart [9].

The constant changes in the generation sector and growing requirements for continuity and certainty of electrical energy supply places a great strain on electric power sector with the need for further transmission network development. Various approaches, such as the use of high temperature low sag conductors, can be employed to increase the transmission

The associate editor coordinating the review of this manuscript and approving it for publication was Yudong Zhang.

capacity of the existing transmission lines [10]. However, these approaches might not provide the long-term solution to the aforementioned challenges. The alternative solution to this problem is the construction of new overhead transmission lines. The development of new overhead transmission lines is subject to numerous administrative, legal, and environmental constraints. Due to the constraints related to safety distances, audible noise levels and the electromagnetic environment, significant challenges are associated with economically developed and densely populated urban areas. The land cost associated with the development of new transmission lines can significantly affect the economic viability of these projects [11]–[13]. Another potential solution is the use of underground cables. This solution is not always applicable and brings with itself specific construction challenges and increased installation and maintenance costs [14]. The construction of multi-circuit overhead transmission lines can increase the unit line corridor transportation capacity, increase the efficiency of land resource use and lower the construction cost. The effectiveness of multi-circuit overhead transmission lines is increasingly being recognized. Double-circuit and quadruple-circuit overhead transmission lines on same tower are already widely used in many countries. These multi-circuit overhead transmission lines can be of the same voltage levels, but also towers with multiple voltage levels can be encountered [11], [15], [16]. Specific challenges are related to high voltage substations at the entrances of which there are often several parallel overhead transmission lines. It is not uncommon for several of them to be placed together on the same towers at the entrances, due to limited space.

Each of these circuits will cause a magnetic field in its environment, and since these are small distances, the total field in the vicinity of such transmission line will be enlarged with their contributions [17], [18]. This means that fields of significantly higher intensity will appear compared to those that would be generated by all transmission lines individually. Given the prescribed allowable field values, in the design stage and during the operation of power facilities, it is necessary to perform calculations, measurements or prediction of the generated field intensities [17], [19], [20]. The field intensity can be reduced by increasing the height of the towers. However, this is not the optimal solution, as it can cause a significant increase in project costs, more complicated construction and higher maintenance requirements. Therefore, when designing multi-circuit overhead transmission lines, phase sequence arrangement and conductor position optimization should be performed [15], [21].

Overhead transmission line rated voltages are selected to meet the recommendations defined by the relevant international regulations [22]. The 110 kV, 220 kV and 400 kV overhead transmission lines are used in transmission network in Bosnia and Herzegovina [23], and also in numerous other countries as single or multi-circuit overhead transmission lines [12].

According to Biot-Savart law, magnetic flux density produced by overhead transmission lines depends on the transmission line conductors current intensities and the distances between the source points and the arbitrary observation point [24]–[26].

Overhead transmission lines conductor heights are defined with allowed phase to ground clearances, which are determined depending on the voltage level i.e. transmission lines with higher rated voltages require higher permissible conductor heights [27]. Overhead transmission lines with higher rated voltages have larger power capacity and they are usually loaded with higher current intensities. Nevertheless, overhead transmission lines with lower rated voltage can also be loaded with high current intensities. In instances, when overhead transmission lines with lower rated voltages and lower conductor heights are loaded with high current intensities, large magnetic flux density levels are expected in their vicinity and near ground level.

Numerous analytical and numerical methods have been developed in response to the need to calculate the value of the magnetic flux density. Nowadays, numerical methods are predominantly used [28], [29]. There is a need, especially in the case of multi-circuit overhead transmission lines, to develop reliable methods that can determine the magnetic flux density at a desired point in space using only the phase currents and positions of the conductors in space [30].

Artificial neural networks can approximate nonlinear functions and model complex input-output relations and such they are applied to wide range engineering problems [31], [32]. Recently, a method based on the ANNs has been proposed to enable magnetic flux density and electric field intensity estimation in the vicinity of overhead transmission lines. The model is designed to be applied on a single-circuit overhead transmission line [33].

In this paper, a novel method is proposed for estimation of magnetic flux density in the vicinity of multi-circuit overhead transmission lines. The proposed method is able to provide accurate estimates for a wide range of different transmission line conductor configurations. This is one characteristic that the proposed method shares with the method proposed in [33]. However, in order to facilitate accurate magnetic flux density estimation in the vicinity of multi-circuit overhead transmission lines, the proposed neural network model is trained to estimate the real and imaginary values of each individual component of magnetic flux density vector, as opposed to the resultant value, as in [33].

The ANN model is used to provide magnetic flux density estimates that are generated by individual circuits in the multi-circuit overhead transmission line environment. The proposed method is able to integrate these estimates and produce the magnetic flux density estimates that correspond to the multi-circuit overhead transmission lines.

The rest of the paper is organized as follows: In Section II the proposed model for estimation of magnetic flux density in the vicinity of multi-circuit overhead transmission line is described in detail. Section III presents the validation of the proposed method. The validation is done by comparing the results obtained by the proposed method to those obtained

with BS law based method and measurement results. Concluding remarks are given in Section IV.

II. DESCRIPTION OF PROPOSED METHOD

A. ARTIFICIAL NEURAL NETWORKS

Development of ANNs is inspired by the fundamental characteristics and functionality of biological computing machines, i.e. biological brains [34]. Artificial neural networks are able to acquire experiential knowledge by identifying patterns and relationships that exist in the training data and they are able to adapt to a changing environment [35], [36].

Artificial neural networks belong to a class of machine learning algorithms. Machine learning is a branch of artificial intelligence that is defined as ''*the field of study that gives computers the ability to learn without being explicitly programmed*'' [37]. In general, ANNs have the capacity to learn, generalize and recall stored knowledge [38]. Here the term generalization is used to denote the ability of a machine learning model to generate correct outputs for new and previously unseen data, i.e. the instances that were not used to train the model. The ANNs can be trained to model complex and highly nonlinear input/output relations.
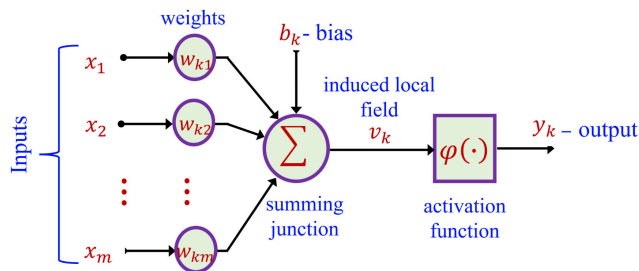

FIGURE 1. A neuron model.

Artificial neural network is a computational model that contains a certain a number of interconnected basic information-processing elements called artificial neurons. Neuron connections are associated with coefficients or synaptic weights that can be adapted by ANN training algorithms. An artificial neuron model is presented in Fig. 1. For some k-th neuron in a neural network architecture with m distinct inputs, a mathematical model of the neuron can be represented by the following equation:

$$y_k = \varphi \left(\sum_{j=1}^{m} w_{kj} \cdot x_j + b_k \right) \tag{1}$$

were, $x_1, x_2, \ldots, x_m$ denote neuron inputs, while $w_{k1}, w_{k2}, \ldots, w_{km}$ represent the associated synaptic weights. The neuron bias is denoted as b_k; the neuron activation function is denoted as $\varphi(\cdot)$ and the output of the k-th neuron is denoted as y_k. The activation function of the k-th neuron maps its activation potential (induced local field), $v_k = \sum_{j=1}^{m} w_{kj} \cdot x_j + b_k$, to neuron output, $y_k = \varphi(v_k)$. In this paper, a nonlinear tan-sigmoid function is selected as an activation function for the

hidden layer neurons. The tan-sigmoid function is described by the following equation [39]:

$$\varphi(v) = \frac{2}{1 + e^{-2v}} - 1 \tag{2}$$

In this paper, a fully connected feed-forward artificial neural network model is developed to estimate magnetic flux density for a range of different transmission line conductor configurations. The graphical illustration of the proposed ANN model is presented in Fig. 2. The ANN architecture consists of 1 input layer, 4 hidden layers and 1 output layer. The input layer consists of 6 inputs. Each hidden layer consists of 20 neurons. Finally, the output layer consists of 4 outputs. The proposed model is designed to provide the magnetic flux density estimate for a given overhead transmission line conductor geometry at a point 1 m above the ground surface and some lateral distance away from the central vertical line.

For the purpose of magnetic flux density estimation, an overhead transmission line configuration is defined by 3 (x, y) points in two dimensional space that denote the geometric description of 3 phase conductors. Instead of 6 coordinate values, the proposed model uses 5 coordinate values to completely describe an overhead transmission line configuration. A coordinate system is defined with respect to the central phase conductor (central vertical line). Specifically, for each considered overhead transmission line configuration, the horizontal coordinate of the central phase conductor is set to zero. Thus, only 5 coordinate values are required to completely describe an overhead transmission line configuration.

In addition to 5 coordinate values that define the geometry of overhead transmission line conductors, every input sample defines the lateral distance of the magnetic flux density estimation point from the central phase conductor. Therefore, the input layer of the proposed ANN model for magnetic flux density estimation consists of six inputs.

On the other hand, the output layer of the proposed ANN model consists of 4 outputs. These four outputs define the real and imaginary parts of magnetic flux density vector components $\underline{B}_x$ and $\underline{B}_y$. The graphical illustration of procedure of obtaining these results by ANN is shown in Fig. 2.

The ANN model is trained using a supervised learning paradigm. Supervised learning techniques are used to develop predictive models based on a training dataset of paired input-output samples, i.e. each training sample in the training dataset is labeled with the desired (ground-truth) output. In this paper, the ANN model training is based on a dataset that represents 200,000 different overhead transmission line conductor configurations. The configurations are generated using a method that is described in detail in [33]. For each of 200,000 different overhead transmission line conductor configurations, the considered dataset includes 201 points with different lateral displacement from the central vertical line. These points are placed at 1 m above the ground surface and range from −100 m to 100 m away from the central vertical line. Thus, the training of the ANN model for magnetic
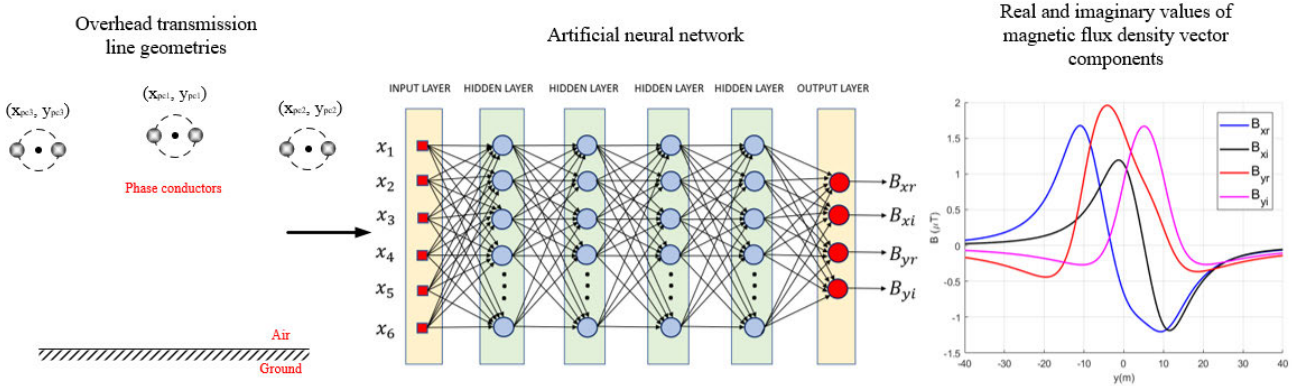
FIGURE 2. Graphical illustration of the proposed ANN model.

flux density estimation is based on a dataset that includes 40,200,000 samples. In this dataset, each sample defines a 6-dimensional input vector and a corresponding 4-dimensional desired (target) vector. The target vectors are obtained using BS based law method under the assumption that in all transmission line phase conductors, current intensity is equal to 100 A. In order to mitigate the overfitting problem, the dataset containing 40,200,000 samples is randomly divided into training (70% samples), validation (15% samples), and testing (15% samples) datasets.

In this paper, the proposed model for magnetic flux density estimation is trained using the scaled conjugate gradient (SCG) algorithm [40]. This is a fast fully-automated algorithm that does not use any critical user-dependent parameters [40]. SCG learning algorithm is designed with the primary objective of avoiding the time-consuming line search that is commonly employed by other conjugate gradient algorithms to evaluate the optimal step size and as such, it is shown to be particularly efficient in instances when the neural network model consists of a large number of free weights [40].

B. BIOT-SAVART LAW BASED METHOD
The target values for all the samples used in the ANN model training, i.e. the desired real and imaginary values of magnetic flux density vector components, are calculated using BS law based method. Specifically, the 2D algorithm of BS law based method is used. This method is also used to validate the proposed magnetic flux density estimation method. The considered BS law based method assumes that source of magnetic flux density are current point sources located at the center of each phase conductor. In the case of bundle phase conductor, the current point source is located at the center of equivalent conductor. According to the BS law based method, x and y component of magnetic flux density vector in an arbitrary point with coordinates (x, y) can be calculated using following equations [41]:

$$\underline{B}_x(x, y) = \sum_{i=1}^{n} \frac{\mu_0 \cdot \underline{I}_i}{2\pi} \cdot \left(-\frac{y - y_i}{r_i^2} + \frac{y + y_i + \alpha}{r_i'^2} \right)$$

$$= B_{xr}(x, y) + j \cdot B_{xi}(x, y) \tag{3}$$

$$\underline{B}_y(x, y) = \sum_{i=1}^{n} \frac{\mu_0 \cdot \underline{I}_i}{2\pi} \cdot \left(\frac{x - x_i}{r_i^2} - \frac{x - x_i}{r_i'^2} \right)$$

$$= B_{yr}(x, y) + j \cdot B_{yi}(x, y) \tag{4}$$

where $\underline{B}_x(x, y)$ and $\underline{B}_y(x, y)$ are x and y vector components of the magnetic flux density phasor at point (x, y), μ_0 is magnetic permeability of air, n is the total number of current point sources, $\underline{I}_i$ is current intensity phasor of i-th point source, (x, y) are coordinates of an arbitrary point, (x_i, y_i) are coordinates of the i-th current point source, α is the complex depth, r_i is the shortest distance between the i-th current point source and arbitrary point, r_i' is the shortest distance between complex image of i-th current point source and arbitrary point, and j is complex unit. The $B_{xr}(x, y)$ and $B_{xi}(x, y)$ represent the real and imaginary values of x component of magnetic flux density vector, while $B_{yr}(x, y)$ and $B_{yi}(x, y)$ represent the real and imaginary values of y component of magnetic flux density vector, respectively. Complex depth is denoted by α and it is defined by following equation [20]:

$$\alpha = \frac{2}{\sqrt{-j \cdot \omega \cdot \mu_0 \cdot (\sigma_{soil} - j \cdot \omega \cdot \varepsilon_{soil})}} \tag{5}$$

where ω is power system angular frequency, σ_{soil} is soil conductivity, ε_{soil} is dielectric permittivity of the soil.

Relevant geometric parameters for the calculation of magnetic flux density are presented in Fig. 3.

C. ESTIMATION RESULTS INTEGRATION
The ANN based method for magnetic flux density estimation presented in [33] is designed to be used for the single-circuit three-phase overhead transmission lines, only. However, in practical situation there is a large number of different multi-circuit overhead transmission line configurations with different number of phase conductors that can be considered. Development of a specific ANN model for each case does not seem like a reasonable solution to address this problem. In order to facilitate the analysis of multi-circuit overhead transmission lines using the ANN approach, a novel ANN model is developed. Unlike the
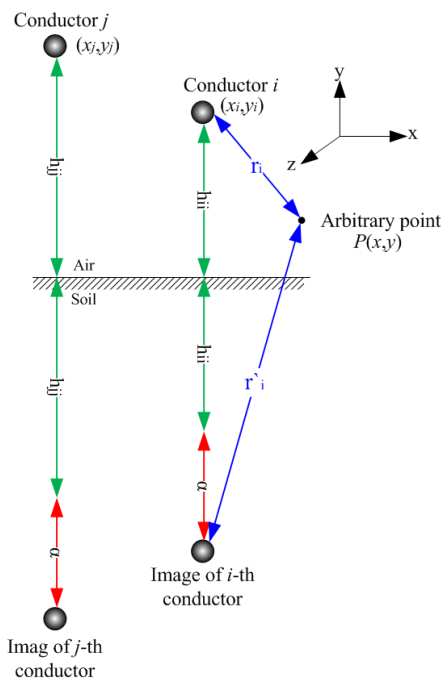
FIGURE 3. Current point source and image of current point source distances from an arbitrary point [33].

model proposed in [33] where the output of the ANN model corresponds to the resultant value of the magnetic flux density $B(x, y)$ at an arbitrary point with coordinates (x, y), in this paper the ANN model is trained to estimate the real and imaginary parts of magnetic flux density vector components $(B_{xr}(x, y), B_{xi}(x, y), B_{yr}(x, y), B_{yi}(x, y))$ at some arbitrary point with coordinates (x, y). The proposed ANN model is designed based on the following considerations:

- the ANN model is trained for a fixed value of applied current intensity,
- the ANN model is trained based on different single-circuit three-phase overhead transmission line configurations,
- the central conductor of the overhead transmission line is placed on the vertical axes.

Having developed the ANN model, as described earlier in this section, the principal problem becomes how to extend its use to the case of multi-circuit overhead transmission lines. In this paper, the following solution is proposed. The estimates of the real and imaginary values of magnetic flux density vector components that are produced by the proposed ANN model correspond to a local coordinate system. The local coordinate system origin coincides with the central phase conductor of that circuit. In order to appropriately account for contributions of the individual circuits to the resultant magnetic flux density, it is necessary to account for the specific spatial locations of the individual circuits with respect to the global coordinates system origin. In relation to the global coordinate system origin, the local coordinate system origin associated with a particular circuit is displaced

only by abscissa. The global coordinate system origin is associated with the center of multi-circuits overhead transmission line. Therefore, the following relations with respect to each output of the ANN model hold:

$$B_{xr,k}(x, y) = B'_{xr}(x - c_k, y) \tag{6}$$

$$B_{xi,k}(x, y) = B'_{xi}(x - c_k, y) \tag{7}$$

$$B_{yr,k}(x, y) = B'_{yr}(x - c_k, y) \tag{8}$$

$$B_{yi,k}(x, y) = B'_{yi}(x - c_k, y) \tag{9}$$

where (x, y) is a point in a multi-circuit overhead transmission line coordinate system. The parameter c_k defines the location of the central phase conductor of k-th circuit on the x-axis with respect to the global coordinate system origin.

The $B'_{xr,k}(x, y)$, $B'_{xi,k}(x, y)$, $B'_{yr,k}(x, y)$, $B'_{yi,k}(x, y)$ denote the ANN output (real and imaginary values of magnetic flux density of x and y vector components of magnetic flux density) associated with the k-th overhead transmission line circuit. The ANN outputs are based on the local coordinate system, where the local coordinate origin coincides with the central phase conductor of the k-th overhead transmission line circuit. On the other hand, $B_{xr,k}(x, y)$, $B_{xi,k}(x, y)$, $B_{yr,k}(x, y)$, $B_{yi,k}(x, y)$ denote the real and imaginary values of magnetic flux density x and y vector components at point (x, y).

Practical multi-circuit overhead transmission lines usually have geometrically identical circuits on opposite sides of the tower. If there are two circuits that are symmetrically placed around tower, then magnetic flux density distribution for both circuits are based on the same ANN outputs. In that case, the ANN model is used to obtain the distributions of the real and imaginary values of magnetic flux density x and y vector components for only one of those circuits.

The ANN model is trained under the assumption that the phase conductors are arranged in such way that the phase angle of the central phase conductor is 0, the phase shift associated with the rightmost phase conductor is $-2\pi/3$ whilst, the phase shift associated with the leftmost conductor is $2\pi/3$. Very often, multi-circuit overhead transmission lines have circuits that are symmetrically placed around the tower but with opposite phase conductor arrangement. In this case, the distribution of the real and imaginary values of magnetic flux density x and y vector components for one circuit can be easily derived from the results associated with the other circuit. Within the local coordinate system, it is necessary to change the sign associated with the real and imaginary parts of y vector component and to rotate the real and imaginary parts of both vector components along the abscissa.

Therefore, phasors of magnetic flux density vector components at an arbitrary point with coordinates (x, y) can be calculated by using following equations:

$$\underline{B}_{xT}(x, y) = \sum_{k=1}^{N} B_{xr,k}(x, y) \cdot \frac{I_k}{I_n} + j \cdot B_{xi,k}(x, y) \cdot \frac{I_k}{I_n} \tag{10}$$

$$\underline{B}_{yT}(x, y) = \sum_{k=1}^{N} B_{yr,k}(x, y) \cdot \frac{I_k}{I_n} + j \cdot B_{yi,k}(x, y) \cdot \frac{I_k}{I_n} \tag{11}$$
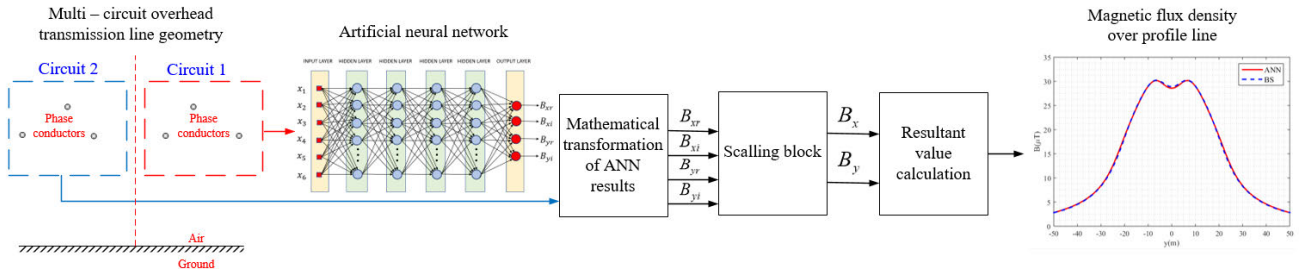
FIGURE 4. Graphical illustration of proposed method for magnetic flux density estimation in vicinity of multi-circuit overhead transmission lines.

where N is total number of circuits of analyzed multi-circuit overhead transmission lines, $\underline{B}_{xT}(x, y)$ and $\underline{B}_{yT}(x, y)$ are x and y components of the magnetic flux density at an arbitrary point (x, y), I_k current intensity of k-th analyzed circuit and I_n is current intensity value that ANN training was based on.

Finally, resultant value of the magnetic flux density at an arbitrary point with coordinates (x, y) can be calculated by using following equation [42]:

$$B(x, y) = \sqrt{\left|\underline{B}_{xT}(x, y)\right|^2 + \left|\underline{B}_{yT}(x, y)\right|^2} \qquad (12)$$

Graphic illustration of the previously described procedure of magnetic flux density estimation in the vicinity of multi-circuit overhead transmission lines is given in Fig. 4.

III. CASE STUDIES
The proposed method for magnetic flux density estimation is evaluated on different multi-circuit overhead transmission lines. The obtained estimates are compared to the calculations made by BS law based method. In addition, the performance of the proposed method has been evaluated on two parallel transmission lines with different rated voltage and applied current intensities. In this case, the performance of the proposed method is compared to BS law based calculations and field measurement results. In all considered cases the magnetic flux density is estimated at a height of 1 m above ground surface, and in increments of 1 m along the lateral profile. The magnetic flux density measurements were performed in an identical manner.

A. COMPARISON WITH CALCULATION RESULTS
The validation of the proposed method is done on different multi-circuit overhead transmission lines and on the parallel single-circuit overhead transmission lines within a common corridor. In this paper, for each considered test case, the estimation of magnetic flux density is based at the point where conductors are closest to the ground level. In fact, the lowest distance of a conductor from the ground is taken as the conductor height. The selected values of the phase conductor heights in the analyzed cases are in accordance with [27].

The first test case corresponds to two identical 400 kV overhead transmission lines with horizontal phase conductor configuration. The central phase conductors of two overhead

transmission lines are 50 m apart along the x-axis. All phase conductors consist of two sub-conductors in a bundle. Both overhead transmission lines have two shield wires and they both have the same phase conductor arrangement. In this case the global coordination system origin is positioned at the middle point between analyzed overhead transmission lines. Geometric parameters of the considered transmission lines are presented in Fig. 5.

For this test case, two scenarios are considered. The first scenario denotes a situation where current intensities of equal magnitude flow in phase conductors of both overhead transmission lines. The second scenario denotes a situation where the applied phase current intensities of overhead transmission line 1 (as shown in Fig. 5) is equal to one half of the applied current intensity of the overhead transmission line 2 (as shown in Fig. 5).

In Fig. 6 the comparison of the results obtained by the proposed magnetic flux density estimation approach and by BS law based method is given. Results presented in Fig. 6a correspond to the first scenario, where the current intensities of all phase conductors are equal to 1200 A on both considered overhead transmission lines. The results presented in Fig. 6b correspond to the second scenario, where the phase current intensity of the overhead transmission line 1 is 600 A and the phase current intensities of the overhead transmission line 2 is 1200 A. For the first scenario, the highest value of the magnetic flux density is at the center of overhead transmission lines and amounts 26.07 μT. Similarly, for the second scenario, the highest value of the magnetic flux density, 26.71 μT, exists at the center of the overhead transmission line with higher applied phase current intensity.

In consideration of the results presented in Fig. 6, it can be noted that for both scenarios, the magnetic flux density estimates obtained using the proposed method closely agree with the calculations obtained using the BS law based method.

The second analysed case in this paper is a double-circuit overhead transmission line of 220 kV rated voltage. The second test case considers two overhead transmission lines with opposite arrangement of the phase conductors. The phase conductor arrangement of each circuit of the analyzed double-circuit overhead transmission line is given in Fig. 7. For this test case, two scenarios are also considered. The first scenario corresponds to the symmetric circuit loading,
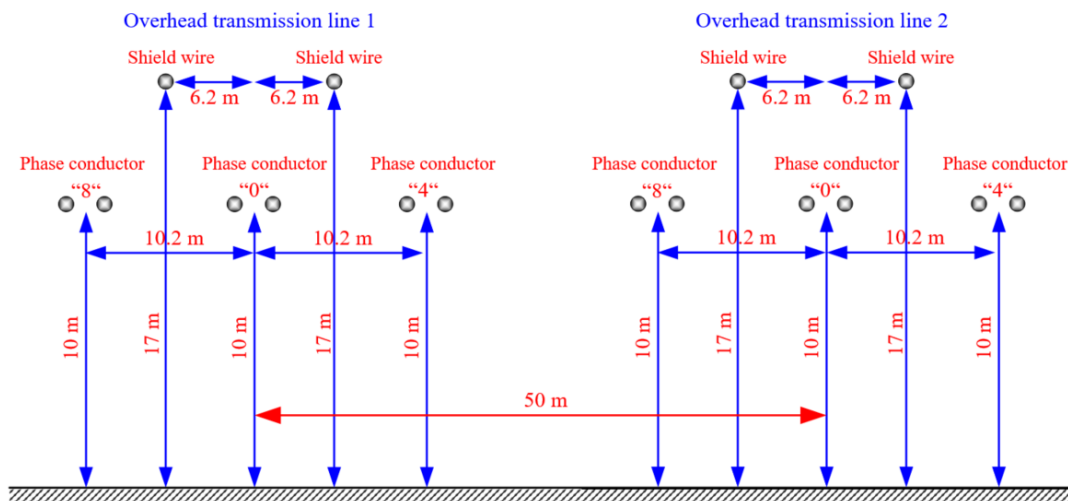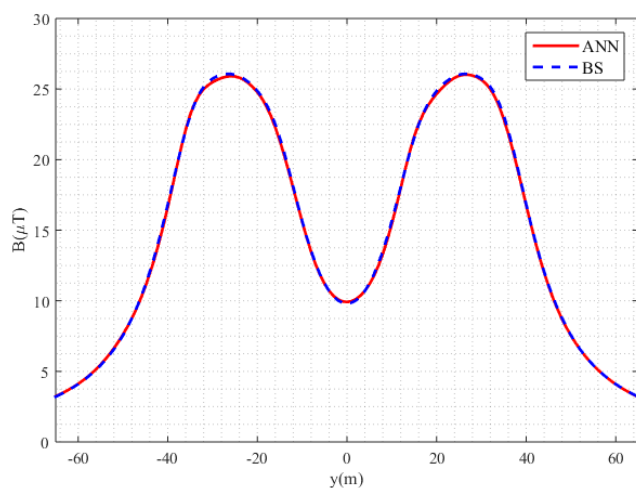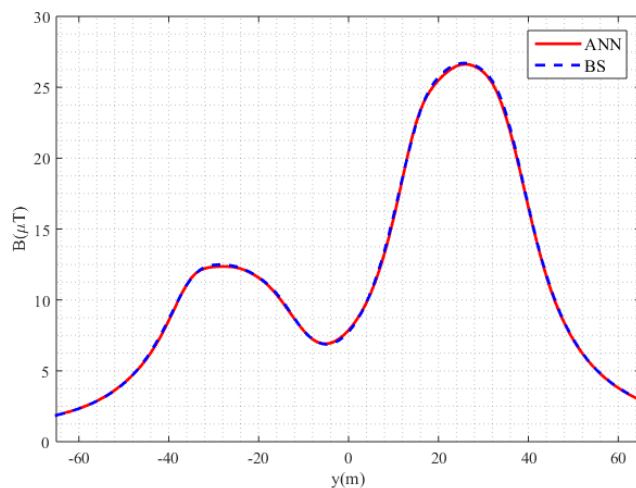
FIGURE 5. Geometry of two horizontal overhead transmission lines of 400 kV rated voltage.

(a) Symmetric scenario

(b) Asymmetric scenario

FIGURE 6. Magnetic flux density distribution of two horizontal overhead transmission lines of 400 kV rated voltage in common corridor.

while the second scenario corresponds to the asymmetric circuit loading. For the first scenario, the two circuits have identical current intensity of 1000 A. On the other hand, for the second asymmetric scenario, the applied current intensity of one circuit is 650 A (Circuit 1), whilst the applied current intensity of the second circuit is 1000 A (Circuit 2).

Due to the geometric symmetry of the analyzed double-circuit overhead transmission line, the proposed ANN model is used to obtain the magnetic flux density estimates for one circuit. The magnetic flux density estimates associated with the other circuit are derived from these estimates. Finally, the results associated with the double-circuit overhead transmission line are obtained by applying the mathematical model described in Section II.

In Fig. 8 the results of magnetic flux density estimation for both analysed scenarios are presented. For the first scenario,

where individual circuits in double-circuit overhead transmission line are symmetrically loaded, the magnetic flux density distribution is presented in Fig. 8a. The highest value of the magnetic flux density on the profile is at the points $x_1 = 8$ m and $x_2 = -8$ m, and amounts 18.68 μT. For the second scenario where individual circuits in double-circuit overhead transmission line are asymmetrically loaded, the estimated magnetic flux density distribution over the considered lateral profile is given in Fig. 8b. Here, the highest value of the magnetic flux density on the profile is at the point $x_1 = 9$ m and amounts 18.2 μT.

The results of magnetic flux density calculations obtained by the BS law based method are shown in Fig. 8 along with the results obtained by the proposed method. The results presented in Fig. 8, demonstrate that the proposed method is able to produce magnetic flux density estimates that closely
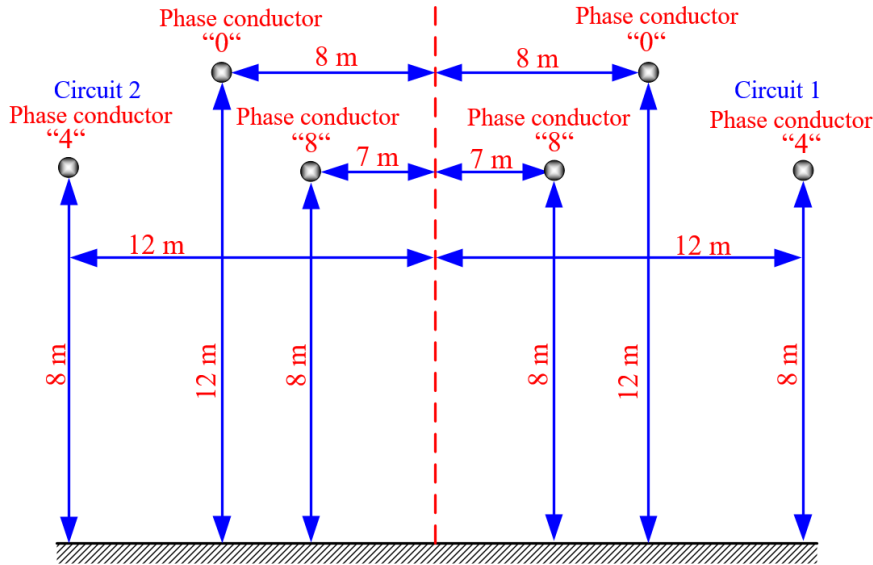
FIGURE 7. Geometry of considered 220 kV double-circuit overhead transmission line.

(a) Symmetric scenario
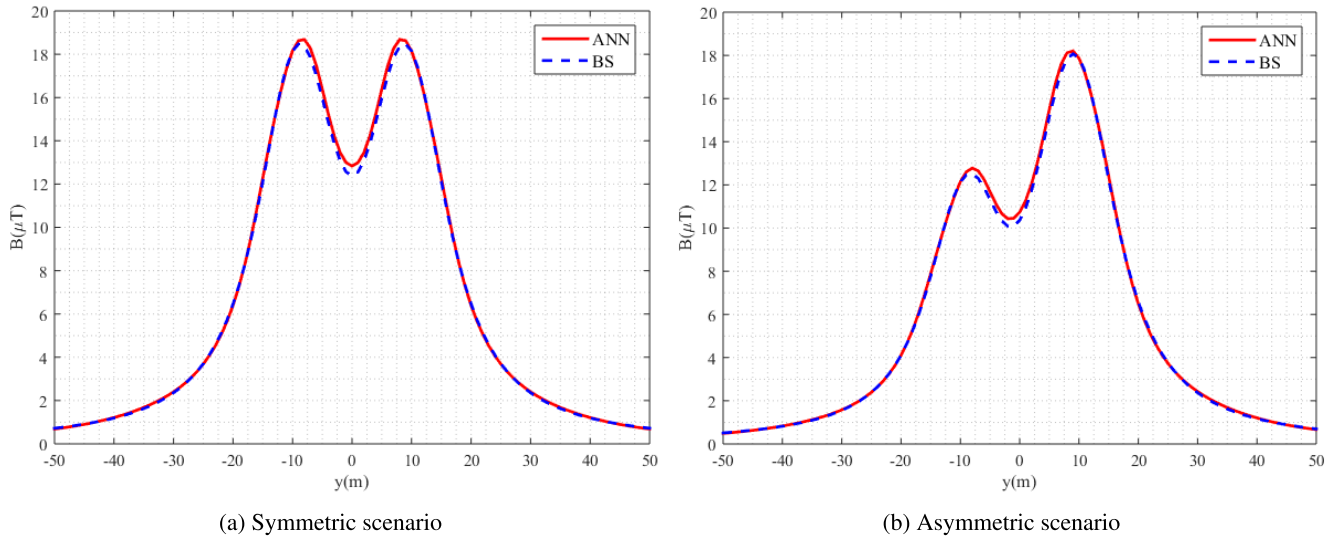
(b) Asymmetric scenario

FIGURE 8. Magnetic flux density distribution in vicinity of 220 kV double-circuit overhead transmission line.

match the calculations obtained using the BS-law based method. Some minor difference between the results obtained by these two methods can be observed only at the center of multi-circuit overhead transmission line.

The third test case corresponds to a quadruple overhead transmission line of E-type with two circuits of 500 kV rated voltage (higher circuits) and two circuits of 220 kV rated voltage [15]. The phase conductor arrangement of the considered quadruple overhead transmission line is given in Fig. 9.

Again, two scenarios are considered. In the first scenario, the applied current intensities for the circuits 3 and 4 (from Fig. 9), are equal 1500 A. Also, the applied current intensities for the circuits 1 and 2 (from Fig. 9), are

equal 1000 A. In the second scenario, the applied current intensities are as follows:

- Circuit 1: 650 A,
- Circuit 2: 1000 A,
- Circuit 3: 1500 A,
- Circuit 4: 1200 A.

The ANN model is used to obtain the real and the imaginary values of magnetic flux density vector components $\underline{B}_x$ and $\underline{B}_y$ for two circuits only, circuit 1 and circuit 3, as shown in Fig. 9. Exploiting the specific relations in the phase conductors arrangement, the magnetic flux density distribution associated with the remaining two circuits is derived from those obtained by the ANN model.
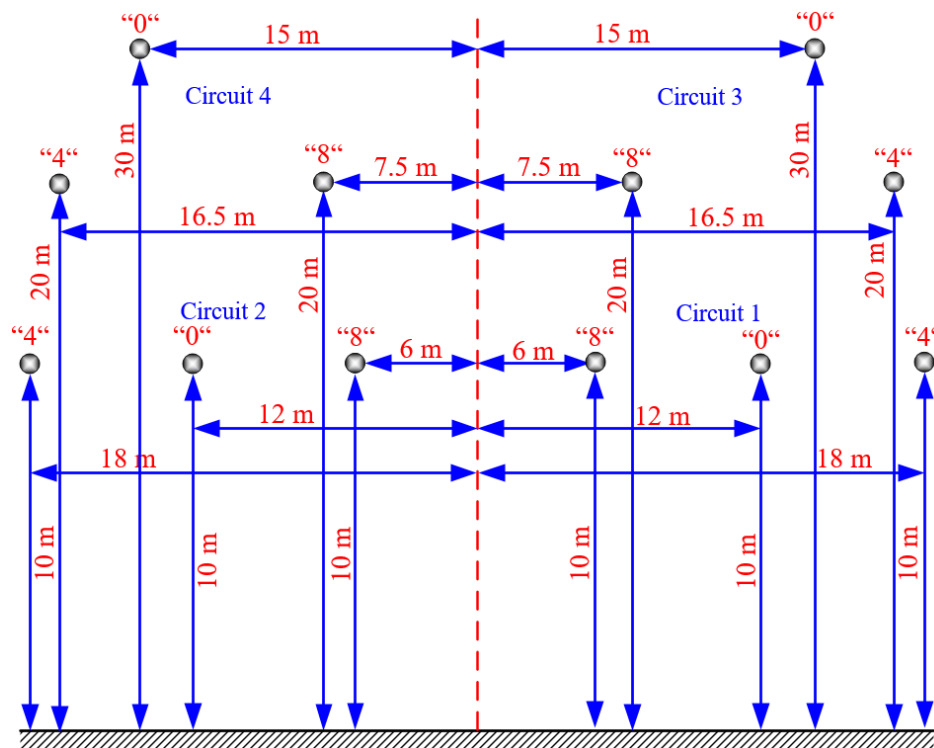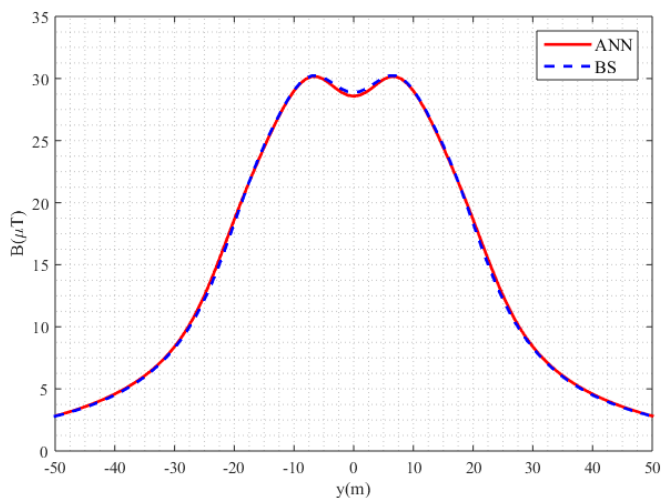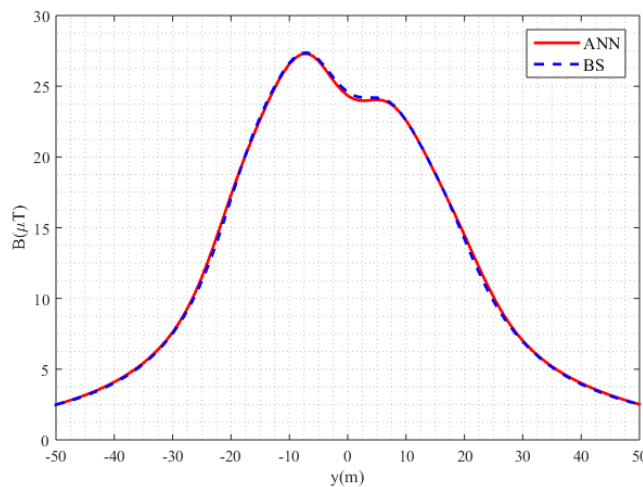
FIGURE 9. Geometry of considered E-type quadruple overhead transmission line.

(a) Symmetric scenario

(b) Asymmetric scenario

FIGURE 10. Magnetic flux density distribution in vicinity of analysed E-type quadruple overhead transmission line.

In Fig. 10 the results of magnetic flux density estimation for both considered scenarios are given. For the first scenario, the estimated magnetic flux density distribution over the considered lateral profile is presented in Fig. 10a. For this scenario, the highest value of the magnetic flux density over the considered lateral profile is at the points $x_1 = 7$ m and $x_2 = -7$ m, and amounts 30.23 μT. On the other hand, the estimated magnetic flux density distribution over the

considered lateral profile for the second scenario, is presented in Fig. 10b. In this case, the highest values of the magnetic flux density on the profile is at the point $x_1 = -7$ m and amounts 27.37 μT.

In addition to the magnetic flux density estimates obtained by the proposed method, the results of magnetic flux density calculations obtained by the BS law based method are shown in Fig. 10. The results in Fig. 10 show that proposed
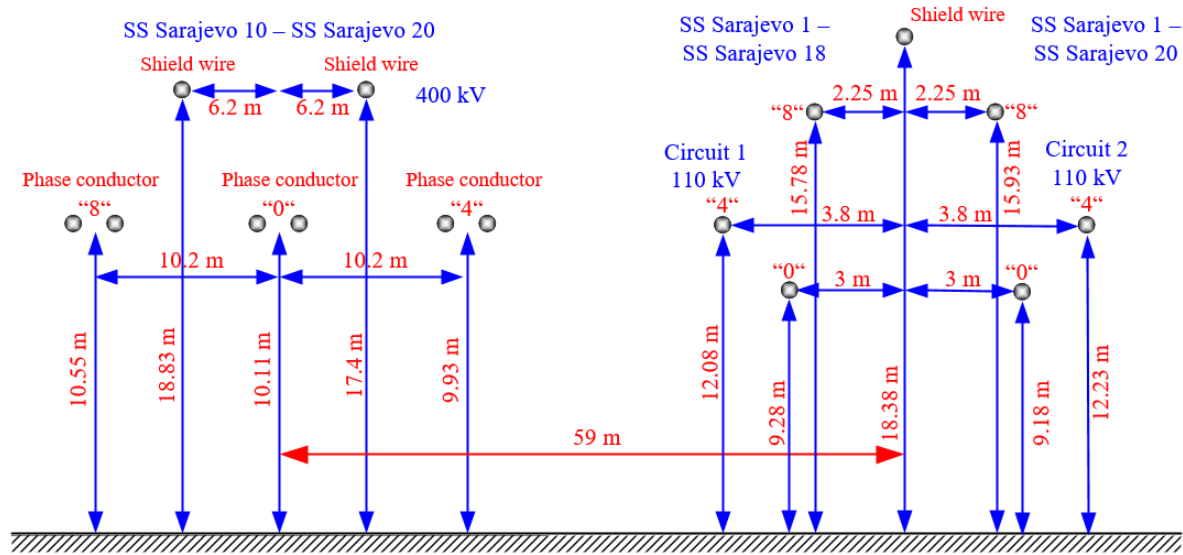
FIGURE 11. Geometry of overhead transmission line of 400 kV rated voltage and one double circuit 110 kV transmission line.

method is able to produce magnetic flux density estimates that closely match the calculations obtained using the BS law based method.

The results obtained on all three test cases demonstrate that the proposed approach can be successfully applied to estimate the magnetic flux density distribution over a lateral profile for different multi-circuit overhead transmission lines.

B. COMPARISON WITH MEASUREMENT RESULTS

The proposed method is also validated with the field measurement results and simultaneously with BS law based method calculation results. Fig. 11 shows the geometry of the considered overhead transmission lines. The considered transmission lines are from electric power system of Bosnia and Herzegovina. The analysis of these transmission lines is based on the measured actual phase current intensities and conductor heights.

On left side of Fig. 11 the 400 kV overhead transmission line substation (SS) Sarajevo 10 - SS Sarajevo 20 is given, while on its right side, the double-circuit 110 kV overhead transmission line is presented. Here, one circuit connects SS Sarajevo 1 - SS Sarajevo 18 and other SS Sarajevo 1 - SS Sarajevo 20. The distance between the two overhead transmission lines vertical axes is 59 m. Overhead transmission line SS Sarajevo 10 - SS Sarajevo 20 has the horizontal configuration of phase conductors and two shield wires. Phase conductors are bundle phase conductors composed of two sub-conductors. On the other hand, double-circuit overhead transmission line SS Sarajevo 1 - SS Sarajevo 18 and SS Sarajevo 1 - SS Sarajevo 20 have a single conductor per phase and have one shield wire. The conductor heights were measured using ultrasonic height meter Suparule model 600, while the horizontal distances between the conductors were taken from the tower specifications obtained from the local

electricity transmission company. The magnetic flux density has been measured using 3D probe Narda - ELT 400. For both analyzed overhead transmission lines, the conductor height and magnetic flux density measurements are conducted at the middle of the span between adjacent transmission line towers. The span of both analyzed overhead transmission lines are almost the same, so this point, for both overhead transmission lines, represents the point closest to ground surface. The phase current intensities were taken from the SCADA system for the period when magnetic flux density were measured. During the measurement of the magnetic flux density the current intensities has varied, as it can be noted from the diagram given in Fig. 12a. The magnetic flux density calculations relied on the following current intensities:

- SS Sarajevo 10 - SS Sarajevo 20: 120.14 A,
- SS Sarajevo 1 - SS Sarajevo 18: 43 A,
- SS Sarajevo 1 - SS Sarajevo 20: 26 A.

Since each circuit in analyzed configuration has different phase conductor heights, magnetic flux density produced by each circuit was estimated separately. These separate results are further used to obtain the resultant magnetic flux density distribution in the vicinity of the analyzed arrangement.

Fig. 12b shows the magnetic flux density estimates obtained by the proposed method as well as the field measurement results and the results produced by the BS law based calculation method. The highest estimated value of the magnetic flux density by the proposed method is 2.667 μT at the center of overhead transmission line of horizontal configuration (SS Sarajevo 10 - SS Sarajevo 20). This is due to the fact that phase current intensity of this overhead transmission line is higher in comparison to the other two.

Also, in this case the obtained results by the proposed method and BS law based method closely match. As it can be noted form Fig. 12, both results deviate from
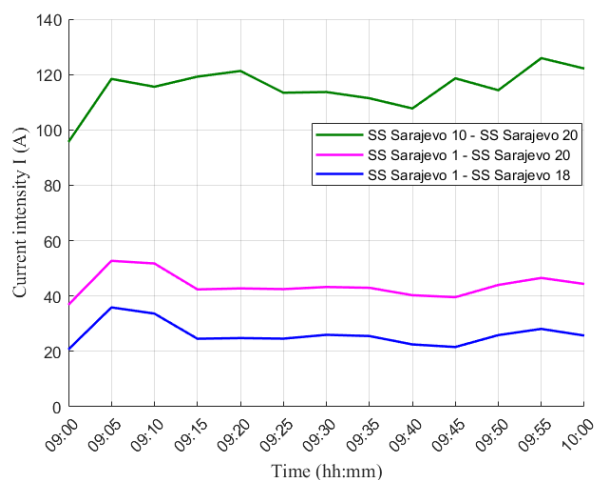
(a) Overhead transmission lines current intensities
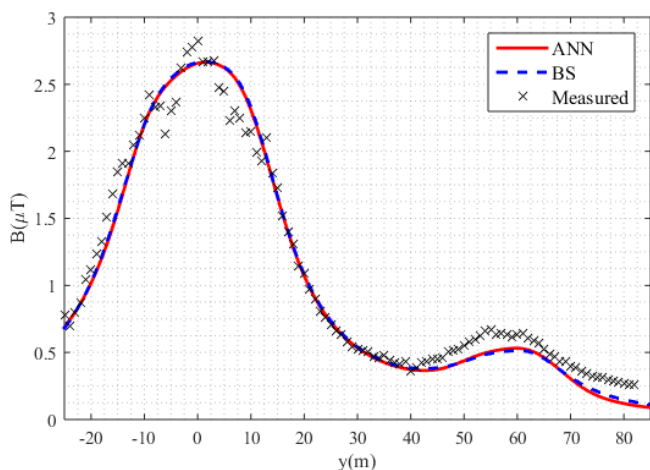
(b) Magnetic flux density distribution

FIGURE 12. Measured current intensities and magnetic flux density distribution of overhead transmission lines under consideration.

measurement results. These deviations are caused by current intensity variation during the period when measurements were made. Furthermore there could have been unbalanced current intensities in the phase conductors of overhead transmission line circuits.

IV. CONCLUSION

In this paper, a novel method for magnetic flux density estimation in the vicinity of multi-circuit overhead transmission lines is presented. The proposed method can be used to analyze the multi-circuit overhead transmission lines where the applied current intensities per circuit are not necessarily equal. This method relies on the ANN model that is trained to estimate the magnetic flux density vector components for a range of single-circuit overhead transmission lines. If the values of the phase current intensities associated with the individual circuits differ from the current intensity used during the ANN training, then appropriate scaling of the ANN outputs is performed.

ANN model is employed to estimate the magnetic flux density distribution for each circuit of a multi-circuit overhead transmission line separately. In cases when there are two or more geometrically identical circuits present in the multi-circuit transmission line, estimations are produced for only one circuit. The magnetic flux density estimates of all other geometrically identical circuits are derived from the previously obtained ANN outputs. The resultant magnetic flux density for the multi-circuit overhead transmission lines is defined in terms of the contributions made by individual single circuit systems. Appropriate transformations are made to account for their different spatial locations. The results of the proposed method are compared to the BS law based method results on different examples of multi-circuit overhead transmission lines.

Based on the example that entails two real parallel overhead transmission lines, with different rated voltages, that are placed in close proximity, the magnetic flux density estimates

obtained by the proposed method are compared to the field measurement results and the calculations obtained by the BS law based method. The obtained results show that the proposed method can be successfully applied to estimate magnetic flux density distribution over the lateral profile for multi-circuit overhead transmission with two or more circuits where the applied current intensities per circuit are not necessarily equal.

In this paper, it was demonstrated that the proposed model is able to accurately estimate magnetic flux density in the vicinity of multi-circuit overhead transmission lines. As such, it can be applied on existing transmission lines, and it can also be used in the design phase of planned overhead transmission lines. The proposed method can be used to evaluate whether the magnetic flux density values associated with the existing or planned overhead transmission lines are within allowable limits.

From the application point of view, the proposed method displays a great deal of flexibility. It can be applied to provide magnetic flux density estimates for a number of different overhead transmission line cases, including: single-circuit overhead transmission line, single-circuits overhead transmission lines in the common corridor and multi-circuit overhead transmission lines with individual circuits being of same or different rated voltage.

REFERENCES

[1] M. Gallastegi, A. Jiménez-Zabala, L. Santa-Marina, J. J. Aurrekoetxea, M. Ayerdi, J. Ibarluzea, H. Kromhout, J. González, and A. Huss, "Exposure to extremely low and intermediate-frequency magnetic and electric fields among children from the INMA-Gipuzkoa cohort," *Environ. Res.*, vol. 157, pp. 190–197, Aug. 2017.

[2] A. T. Amoon *et al.*, "Proximity to overhead power lines and childhood leukaemia: An international pooled analysis," *Brit. J. Cancer*, vol. 119, no. 3, pp. 364–373, Aug. 2018.

[3] C. Sermage-Faure, C. Demoury, J. Rudant, S. Goujon-Bellec, A. Guyot-Goubin, F. Deschamps, D. Hemon, and J. Clavel, "Childhood leukaemia close to high-voltage power lines—The Geocap study 2002–2007," *Brit. J. Cancer*, vol. 108, pp. 1899–1906, Apr. 2013.

[4] C. M. Crespi, J. Swanson, X. P. Vergara, and L. Kheifets, "Childhood leukemia risk in the California power line study: Magnetic fields versus distance from power lines," *Environ. Res.*, vol. 171, pp. 530–535, Apr. 2019.

[5] C. Pedersen, C. Johansen, J. Schüz, J. H. Olsen, and O. Raaschou-Nielsen, "Residential exposure to extremely low-frequency magnetic fields and risk of childhood leukaemia, CNS tumour and lymphoma in Denmark," *Brit. J. Cancer*, vol. 113, no. 9, pp. 1370–1374, Nov. 2015.

[6] A. Karimi, F. G. Moghaddam, and M. Valipour, "Insights in the biology of extremely low-frequency magnetic fields exposure on human health," *Mol. Biol. Rep.*, vol. 47, no. 7, pp. 5621–5633, Jul. 2020.

[7] IARC Working Group on the Evaluation of Carcinogenic Risks to Humans, World Health Organization, and International Agency for Research on Cancer, *Non-Ionizing Radiation. Part 1: Static and Extremely Low-Frequency (ELF) Electric and Magnetic Fields* (IARC Monographs on the Evaluation of Carcinogenic Risks to Humans), vol. 80. Lyon, France: IARC Press, 2002.

[8] J. Lin, R. Saunders, K. Schulmeister, P. Söderberg, B. Stuck, A. Swerdlow, M. Taki, B. Veyret, G. Ziegelberger, M. Repacholi, R. Matthes, A. Ahlbom, K. Jokela, and C. Roy, "ICNIRP Guidelines for limiting exposure to time-varying electric and magnetic fields (1 Hz to 100 kHz)," *Health Phys.*, vol. 99, pp. 818–836, Jan. 2010.

[9] E. Lunca, S. Ursache, and A. Salceanu, "Computation and analysis of the extremely low frequency electric and magnetic fields generated by two designs of 400 kV overhead transmission lines," *Measurement*, vol. 124, pp. 197–204, Aug. 2018.

[10] J.-R. Riba, S. Bogarra, Á. Gómez-Pau, and M. Moreno-Eguilaz, "Uprating of transmission lines by means of HTLS conductors for a sustainable growth: Challenges, opportunities, and research needs," *Renew. Sustain. Energy Rev.*, vol. 134, Dec. 2020, Art. no. 110334.

[11] J. S. Acosta and M. C. Tavares, "Optimal selection and positioning of conductors in multi-circuit overhead transmission lines using evolutionary computing," *Electr. Power Syst. Res.*, vol. 180, Mar. 2020, Art. no. 106174.

[12] A. Dziendziel, H. Kocot, and P. Kubek, "Construction and modeling of multi-circuit multi-voltage HVAC transmission lines," *Energies*, vol. 14, no. 2, p. 421, Jan. 2021.

[13] J. S. Acosta and M. C. Tavares, "Methodology for optimizing the capacity and costs of overhead transmission lines by modifying their bundle geometry," *Electr. Power Syst. Res.*, vol. 163, pp. 668–677, Oct. 2018.

[14] K. Król and W. Machczynski, "Optimization of electric and magnetic field intensities in proximity of power lines using genetic and particle swarm algorithms," *Arch. Electr. Eng.*, vol. 67, no. 4, pp. 829–843, Jul. 2018.

[15] W. Liu, K. Liu, M. Pan, and G. Xu, "Research on electromagnetic character of 500/220 kV mixed-voltage quadruple-circuit transmission line," in *Proc. 12th Int. Conf. Environ. Electr. Eng.*, May 2013, pp. 227–231.

[16] B. Li, W. Wang, W. Wen, B. Yao, J. He, and X. Wang, "Unbalanced currents of EHV multi-circuit lines and coordination of zero-sequence over-current relayings," *Int. J. Electr. Power Energy Syst.*, vol. 126, Mar. 2021, Art. no. 106607.

[17] R. Deltuva and R. Lukočius, "Distribution of magnetic field in 400 kV double-circuit transmission lines," *Appl. Sci.*, vol. 10, no. 9, p. 3266, May 2020.

[18] A. Dahab, F. Amoura, and W. Abu-Elhaija, "Comparison of magnetic-field distribution of noncompact and compact parallel transmission-line configurations," *IEEE Trans. Power Del.*, vol. 20, no. 3, pp. 2114–2118, Jul. 2005.

[19] C. P. Nicolaou, A. P. Papadakis, P. A. Razis, G. A. Kyriacou, and J. N. Sahalos, "Measurements and predictions of electric and magnetic fields from power lines," *Electr. Power Syst. Res.*, vol. 81, no. 5, pp. 1107–1116, May 2011.

[20] J. C. Salari, A. Mpalantinos, and J. I. Silva, "Comparative analysis of 2- and 3-D methods for computing electric and magnetic fields generated by overhead transmission lines," *IEEE Trans. Power Del.*, vol. 24, no. 1, pp. 338–344, Jan. 2009.

[21] G. Feng, Y. Wang, and B. Zhang, "Study on electromagnetic environment of multi-circuit transmission lines on same tower," in *Proc. Joint Int. Conf. Power Syst. Technol. IEEE Power India Conf.*, Oct. 2008, pp. 1–5.

[22] *IEC Standard Voltages*, Standard IEC 60038:2009, International Electrotechnical Commission, 2009.

[23] *Grid Code*, Independ. Syst. Oper. (ISO), Bosnia and Herzegovina, 2019.

[24] H. M. Ismail, "Effect of tower displacement of parallel transmission lines on the magnetic field distribution," *IEEE Trans. Power Del.*, vol. 23, no. 4, pp. 1705–1712, Oct. 2008.

[25] A. Z. El Dein, "Magnetic-field calculation under EHV transmission lines for more realistic cases," *IEEE Trans. Power Del.*, vol. 24, no. 4, pp. 2214–2222, Oct. 2009.

[26] A. Diamantis and A. G. Kladas, "Mixed numerical methodology for evaluation of low-frequency electric and magnetic fields near power facilities," *IEEE Trans. Magn.*, vol. 55, no. 6, pp. 1–4, Jun. 2019.

[27] *Overhead Electrical Lines Exceeding AC 1 kV—Part 1: General Requirements—Common Specifications*, European Standard EN 50341-1:2012, 2012.

[28] T. Modric, S. Vujevic, and D. Lovric, "3D computation of the power lines magnetic field," *Prog. Electromagn. Res.*, vol. 41, pp. 1–9, 2015.

[29] S. Vujevic and T. Modric, "The influence of conductive passive parts on the magnetic flux density produced by overhead power lines," *Facta Univ., Electron. Energetics*, vol. 32, no. 4, pp. 555–569, 2019.

[30] F. Muñoz, J. A. Aguado, F. Martín, J. J. López, A. Rodríguez, J. B. García, A. R. Treitero, and R. Molina, "An intelligent computing technique to estimate the magnetic field generated by overhead transmission lines using a hybrid GA-Sx algorithm," *Int. J. Electr. Power Energy Syst.*, vol. 53, pp. 43–53, Dec. 2013.

[31] Z. Zhao, Z. Wang, J. Yuan, J. Ma, Z. He, Y. Xu, X. Shen, and L. Zhu, "Development of a novel feedforward neural network model based on controllable parameters for predicting effluent total nitrogen," *Engineering*, vol. 7, no. 2, pp. 195–202, Feb. 2021.

[32] X. Qi, G. Chen, Y. Li, X. Cheng, and C. Li, "Applying neural-network-based machine learning to additive manufacturing: Current applications, challenges, and future perspectives," *Engineering*, vol. 5, no. 4, pp. 721–729, Aug. 2019.

[33] A. Alihodzic, A. Mujezinovic, and E. Turajlic, "Electric and magnetic field estimation under overhead transmission lines using artificial neural networks," *IEEE Access*, vol. 9, pp. 105876–105891, 2021.

[34] D. D. Cox and T. Dean, "Neural networks and neuroscience-inspired computer vision," *Current Biol.*, vol. 24, no. 18, pp. R921–R929, Sep. 2014.

[35] G. E. Hinton, "How neural networks learn from experience," *Sci. Amer.*, vol. 267, no. 3, pp. 144–151, Sep. 1992.

[36] S. Agatonovic-Kustrin and R. Beresford, "Basic concepts of artificial neural network (ANN) modeling and its application in pharmaceutical research," *J. Pharmaceutical Biomed. Anal.*, vol. 22, no. 5, pp. 717–727, 2000.

[37] A. L. Samuel, "Some studies in machine learning using the game of checkers," *IBM J. Res. Develop.*, vol. 3, no. 3, pp. 210–229, Jul. 1959.

[38] S. Haykin, *Neural Networks and Learning Machines*, 3rd ed. London, U.K.: Pearson, 2009.

[39] M. Dorofki, A. H. Elshafie, O. Jaafar, O. A. Karim, and S. Mastura, "Comparison of artificial neural network transfer functions abilities to simulate extreme runoff data," *Int. Proc. Chem., Biol. Environ. Eng.*, vol. 33, pp. 39–44, May 2012.

[40] M. F. Møller, "A scaled conjugate gradient algorithm for fast supervised learning," *Neural Netw.*, vol. 6, no. 4, pp. 525–533, Jan. 1993.

[41] J. A. B. Faria and M. E. Almeida, "Accurate calculation of magnetic-field intensity due to overhead power lines with or without mitigation loops with or without capacitor compensation," *IEEE Trans. Power Del.*, vol. 22, no. 2, pp. 951–959, Apr. 2007.

[42] A. Mujezinovic, N. Dautbasic, and M. M. Dedovic, "More accurate 2D algorithm for magnetic field calculation under overhead transmission lines," in *Advanced Technologies, Systems, and Applications IV—Proceedings of the International Symposium on Innovative and Interdisciplinary Applications of Advanced Technologies (IAT 2019)*. Cham, Switzerland: Springer, 2019.

ADNAN MUJEZINOVIC (Member, IEEE) received the M.Sc. and Ph.D. degrees in electrical engineering from the Faculty of Electrical Engineering, University of Sarajevo, Bosnia and Herzegovina, in 2011 and 2017, respectively. Since 2012, he has been with the Faculty of Electrical Engineering as a Teaching Assistant and currently an Associate Professor. He has authored numerous conferences and journal articles. His research interests include numerical calculations of electromagnetic fields, cathodic protection, and transmission lines.

EMIR TURAJLIC (Member, IEEE) received the Ph.D. degree from Brunel University, U.K., in 2007. He is currently an Associate Professor with the Department of Telecommunications, Faculty of Electrical Engineering, University of Sarajevo, Bosnia and Herzegovina. He has authored numerous conferences and journal articles. He has written books on artificial neural networks and image and video compression. His research interests include the fields of digital signal processing, speech processing, artificial intelligence, machine learning, image processing, data compression, and metaheuristic algorithms.

NEDIS DAUTBASIC was born in Srebrenica, Bosnia and Herzegovina. He received the B.Sc. and M.Sc. degrees in electrical engineering from the Faculty of Electrical Engineering, University of Sarajevo. He is currently pursuing the Ph.D. degree with International Burch University. He works with the Faculty of Electrical Engineering, University of Sarajevo, as a Teaching Assistant. His research interests include power system analysis, electromagnetic transients, grounding systems, and signal processing.

AJDIN ALIHODZIC (Member, IEEE) received the B.S. and M.S. degrees from the Department for Electric Power Engineering, Faculty of Electrical Engineering, University of Sarajevo, in 2015 and 2017, respectively, where he is currently pursuing the Ph.D. degree. From 2017 to 2020, he was an Investment Associate Engineer in the Executive Directorate for Investments at Joint Stock Company BH Telecom. Since 2020, he has been a Teaching Assistant with the University of Sarajevo. His research interests include numerical techniques in electromagnetics, transmission lines, and artificial intelligence.

MAJA MUFTIC DEDOVIC was born in Sarajevo, Bosnia and Herzegovina. She received the B.Sc. and M.Sc. degrees in electrical engineering from the Faculty of Electrical Engineering, University of Sarajevo, where she is currently pursuing the Ph.D. degree with the Faculty of Electrical Engineering. She works with the Faculty of Electrical Engineering, University of Sarajevo, as a Teaching Assistant. Her research interests include power system analysis, power system dynamics and stability, WAMPCS, and signal processing.

● ● ●